Glass Formation, Ionic Conductivity, and Conductivity/Viscosity Decoupling, in $LiAlCl_4$ + $LiClO_4$ and $LiAlCl_4$ + $LiAlCl_3$·Imide Solutions

M. Videa and C. A. Angell*

Department of Chemistry, Arizona State University, Tempe, Arizona 85287-1604

Received: October 30, 1998; In Final Form: February 16, 1999

As part of a search for chemically and electrochemically stable ambient temperature molten lithium salt systems, we have investigated the properties of solutions of $LiAlCl_4$ with various second components. In this paper we review the factors which determine the ambient temperature conductivity and report results for two systems, one of which satisfies the stability requirements although failing to provide the high conductivities which are needed for a successful ambient temperature Li battery electrolyte. These ionic solutions appear to be very fragile liquids. Evidence is found for a mixing incompatibility of polarizable and nonpolarizable components of binary melts.

Introduction

Fast energy delivery devices such as lithium batteries demand an optimum transport rate of lithium ions from anode to cathode without polarization problems. This requirement is achieved when the ionic conductivity of the electrolyte is supported by a highly mobile cation with a transport number close to unity.

In a recent report[1] it was shown that various lithium salt systems could be retained in the supercooled liquid state at ambient temperature and that certain of these exhibited exceptionally high electrical conductivities, as high as 10^{-2} S cm^{-1} at 25 °C. Furthermore it appeared that these electrolytes would exhibit high cationic transport numbers which would make them attractive for rechargeable cell applications. The problem with the systems described, as far as their application to lithium battery technology is concerned, is that they contain chemically unstable components such as ClO_4^-. Consequently we have been attempting to find combinations of lithium salts which would combine the ambient temperature stability and high conductivity of these systems with chemical and electrochemical stability. While this proves to be a formidable task,[2] some interesting molten salt chemistry and liquid state phenomenology is being revealed in the course of investigation. Some examples are reported in the present paper.

Two factors can contribute to the establishment of a high ambient temperature conductivity in an ionic liquid. The first factor is a high fluidity. The second is a high conductivity/viscosity decoupling index,[3,4] which means that at any temperature, the probability of small ion motion is much greater than that of a viscous flow event. Each of these factors will now be discussed in some detail.

The main requirement for a high ambient temperature fluidity is a low glass transition temperature T_g (usually thought of as the temperature where viscosity is 10^{13} poise). The fluidity Ø [= (viscosity)$^{-1}$] at a given temperature interval above T_g will, however, be enhanced if the liquid exhibits a high fragility[5] which means that the fluidity exhibits a strongly non-Arrhenius temperature dependence such that it rises rapidly with increase of temperature above T_g. This occurs if the parameter D in the modified[5] Vogel−Fulcher−Tammann equation,[6] eq 1 below, is small. This equation is the most successful of a variety of three-parameter equations[7] which have been proposed to describe the deviations from Arrhenius behavior found for liquids which fail to crystallize during cooling. It is usually written

$$Ø = Ø_o \exp[DT_o/(T - T_o)] \quad (1)$$

where $Ø_o$, D, and T_o are constants and the units are reciprocal poise. T_o itself, which appears as a low-temperature limit or ground-state temperature, can be obtained from extrapolations of thermodynamic data.[8] The interpretation of eq 1 in terms of non zero K ground state is controversial and can be avoided if eq 1 is replaced by the double exponential relation[9]

$$Ø = Ø_o \exp -[1 + \exp(\Delta H^* - T\Delta S^*/RT)] \quad (2)$$

in which ΔH^* and ΔS^* are thermodynamic parameters. In eq 2, ΔH^* and ΔS^* are the parameters governing the fundamental configurational excitation process in the liquid[10,11] and they determine the thermodynamic properties such as heat capacity.[10] ΔH* correlates with the parameter T_o of eq 1 while ΔS^*, the entropy change accompanying an elementary excitation, controls the fragility[11] and hence plays the role of D in eq 1. The data-fitting abilities of eqs 1 and 2 are comparable.

Now it is a matter of experience that in a given ionic liquid, the probability of irreversible movement of a small low-charged cation is higher than that of the larger group of particles involved in a viscous flow event.[3,4] In fact, knowledge of this decoupling goes back to the early days of molten salt chemistry when violations of the Walden rule connecting conductivity and viscosity were recognized and the fractional Walden rule[12] was formulated

$$\Lambda\eta^\gamma = \sigma V_m \eta^\gamma = \text{const} \quad (3)$$

where Λ is the equivalent conductivity, η is the viscosity, σ is the specific conductivity, V_m is the molar volume, and γ is a constant $0 < \gamma < 1.0$. This found an easy interpretation in terms of transition state theory in which the activation energy for conductivity had a smaller value than the activation energy for viscosity. In terms of eq 2 this requires the parameter D to be smaller for conductivity than for viscosity, as has been known to be the case for a long time.[13] In eq 2 it requires a parameter,

* Author to whom correspondence should be addressed.

10.1021/jp984276t CCC: $18.00
Published on Web 04/09/1999

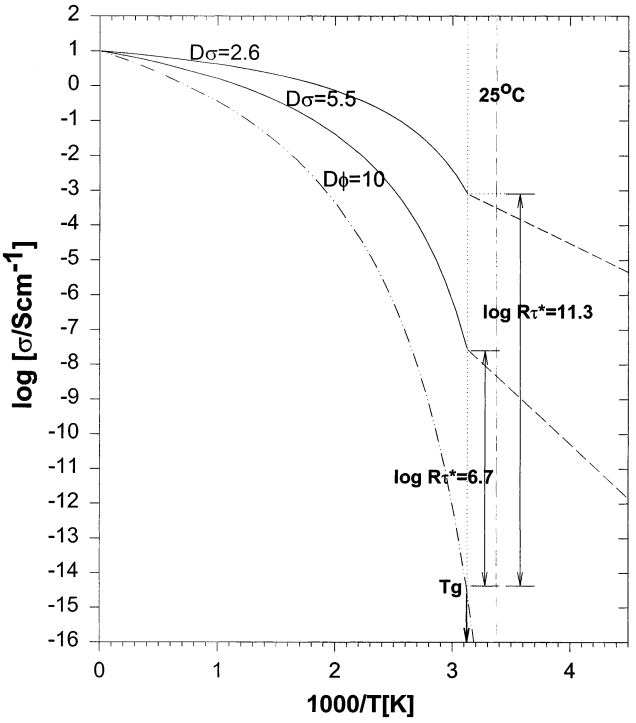

Figure 1. Demonstration of how the value of the eq 1 parameter D_σ for a mobile species (in a melt whose structural relaxation is controlled by a parameter $D_\eta = 10$ can affect the value of conductivity at the glass transition temperature, T_g, hence will determine the material constant log R_τ*. Knowledge of this constant allows the conductivity at other temperatures to be predicted from the value of T_g because the glass conductivity has an Arrhenius temperature dependence with a pre-exponent of $\sim 10^2$ S cm^{-1}.

ζ, to be included to account for the different probabilities of the two dynamic processes in a liquid fixed in a single thermodynamic state. Then eq 2 becomes

$$P\mathrm{i} = P_\mathrm{o} \exp \zeta_\mathrm{p}/[1 + \exp(\Delta H^* - \mathrm{T}\Delta S^*/\mathrm{RT})] \qquad (4)$$

where P is the property under study, and $\mathrm{O} < \zeta_\mathrm{P} < 1$. P may be fluidity Ø, conductivity σ, diffusivity D_i, reciprocal relaxation time τ^{-1}, etc.

Since the conductivity is itself determined by the individual ionic contributions, the fundamental breakdown involved in the decoupling phenomenon is that between diffusivity and viscosity which has been contained in the Stokes−Einstein equation. The basis for the Stokes−Einstein equation is that the frictional force impeding the motion of an ion in a fluid is the viscous force, a force which is proportional to the size of the moving particle and the shear viscosity. It is the breakdown of the Stokes−Einstein equation for small singly charged ions in viscous melts that is the reason that the extensively studied superionic glasses[4,14−17] can exist. The breakdown is quantified by the decoupling index[4] R_τ.

R_τ is defined by the ratio of the structural relaxation time to the conductivity relaxation time, τ_s/τ_σ.[3,4] At the glass transition temperature T_g determined by differential scanning calorimetry conducted at 10 K/min, the structural relaxation time is always about 100 s and equal to the enthalpy relaxation time.[18] Thus a measurement of the conductivity at the glass transition temperature permits the decoupling index at T_g, R_τ^*, to be obtained, with minimum effort, from the approximate relationship,[4]

$$R_\tau^* = 2 \times 10^{14} \sigma_{\mathrm{dc}(T_g)} \qquad (5)$$

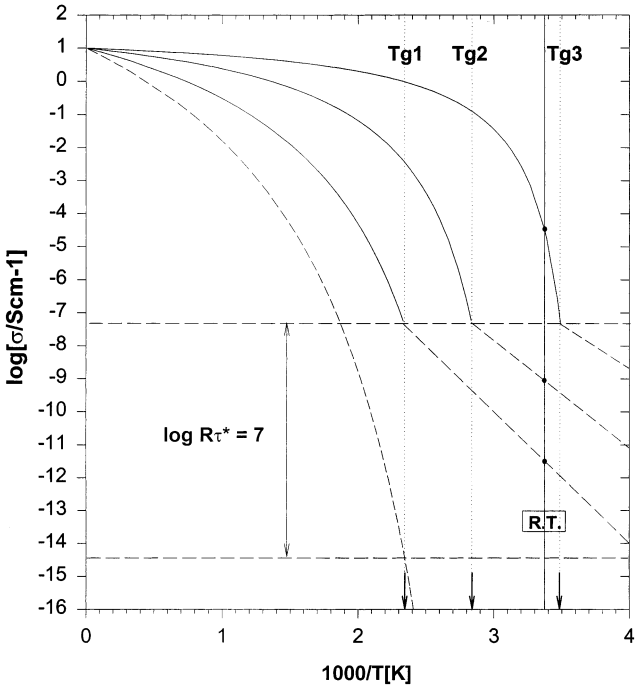

Figure 2. Demonstration of the effect of the value of T_g, for glasses of fixed log R_τ* value, on the ambient temperature conductivity. For case 2, T_g was lowered by changing the D_η parameter in eq 2. For case 3 it was lowered by changing the T_o value.

where $\sigma_{\mathrm{dc}(T_g)}$ is the dc conductivity at the glass transition temperature and the dimensions of the constant term cancel those of σ. Figures 1 and 2, which are constructed using different parametrizations of eq 1, allow the effects of these different factors to be clearly displayed. Figure 1 shows the effect of making the eq 1 D value smaller than the initial value $D_\sigma = D_\eta = 10$ (dashed curve), while keeping τ_o and T_o constant. It results in the conductivity at the temperature T_g becoming higher and, as a result, the ambient temperature conductivity (σ_{25}) becoming higher. The decoupling index R_τ, in log units, increases a little less rapidly than the value of D decreases. Figure 2 shows that, when D_σ and D_η remain fixed, so that the decoupling index is constant, the conductivity at ambient can be increased if T_g is decreased. Usually decreases in T_g will be due to decreases in T_o associated with the presence of larger ions which reduce the coulomb cohesion. However, it could also arise if D_η is decreased at constant T_o (i.e., by increase of fragility) because from eq 1 this will also decrease the temperature at which the fluidity reaches 10^{-13} poise, and the glass transition occurs.

One aim of research, then, is to discover the factors that determine R_τ, on one hand, and T_g and fragility on the other for liquid salt mixtures which do not crystallize at ambient temperature. Another is to determine the conditions of composition which inhibit or prevent crystallization of salts, making ambient temperature liquids or glasses possible in the first place. This paper reports some progress in the direction of realizing each of these aims.

Experimental Section

Materials. Anhydrous AR $LiClO_4$ was obtained from Aldrich and was used without further purification. Li bis-(trifluoromethane sulfonyl) imide, (Li "imide") was obtained gratis from 3M Co.

$LiAlCl_4$ was prepared by heating drybox-weighed quantities of anhydrous LiCl from Aldrich with purified $AlCl_3$ obtained by vacuum sublimation of the anhydrous $AlCl_3$ provided by

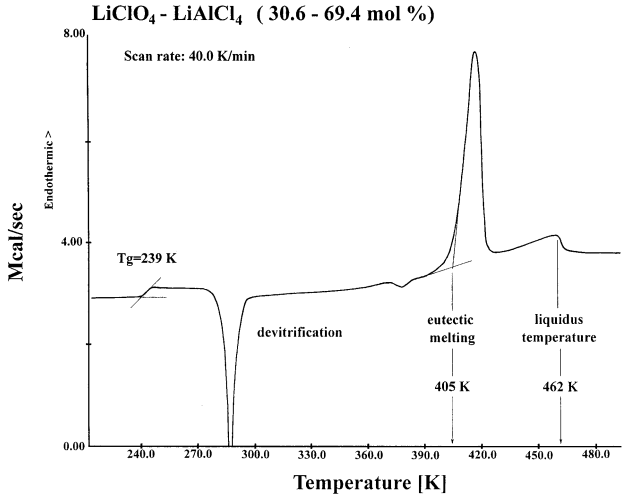

Figure 3. DSC thermogram, obtained at 40 K/min scan rate, of a sample of quenched $LiClO_4$ + $LiAlCl_4$ solution, showing thermal effects due to the glass transition, crystallization eutectic melting, and liquidus (end of melting). Samples were quenched inside the instrument at a rate of 300 K/min.

Aldrich Co. The liquid product was transparent, colorless, and free of suspended material.

Solutions of $LiAlCl_4$ and $LiClO_4$ on one hand, and of $LiAlCl_4$ and Li imide on the other, were prepared by drybox weighing and fusion of the components.

The solvents propylene carbonate and DMSO for binary solution determinations of T_g were obtained from Aldrich Co.

Glass transition temperatures and liquidus temperatures were determined using differential scanning calorimetry (Perkin-Elmer DSC-4).

Conductivities were determined from complex impedance data obtained using the automated HP 4192A frequency analyzer system described in previous papers.[19] Samples were contained in small twin Pt wire dip-type cells, the cell constants of which were determined using standard KCl solution.

Results

Figure 3 shows a typical DSC scan from which glass transition temperatures, T_g, crystallization temperatures, T_c, eutectic temperatures, T_e, and liquidus temperatures, T_l, are obtained by the dashed line constructions shown in the figure. Data of this kind were then used to obtain the T_g vs composition plots of Figure 4, and to construct the phase diagrams shown in Figure 5 and Figure 6.

The results of the T_g measurements for a variety of lithium salts which are not glass-forming by themselves are shown in the right-hand side of Figure 2 where they are juxtaposed with the earlier results on binary salt solutions reported in ref 1. It is seen that the extrapolations of the two different types of solutions support each other reasonably well. The lowest T_g values observed in Figure 4 are those of salts with the Cl(VII) and Cl(V) oxyanions, i.e., $LiClO_4$ and $LiClO_3$, presumably because the oxygen electrons are so polarized toward (or orbitally mixed with) the central chlorine that the surface charge density is like that of a large anion with its charge at the center. The contrast between the T_g values of $LiClO_4$ and $LiBF_4$, in which the physical size of the anions is the same but the F^- polarizability much less, supports this interpretation.

To obtain lower T_g values the size of the anion must be increased. $LiAlCl_4$ cannot be studied in the molten salt or salt/solvent solutions of Figure 4 because it decomposes the solvent, but the glassy state may be observed in solutions with $LiClO_4$, as seen in Figure 3. The results of Figure 3 type scans for a variety of solutions in this binary $LiClO_4$−$LiAlCl_4$ system are shown in Figure 5. The system shows only a narrow region of glass-forming ability on the $LiClO_4$-rich side of the eutectic

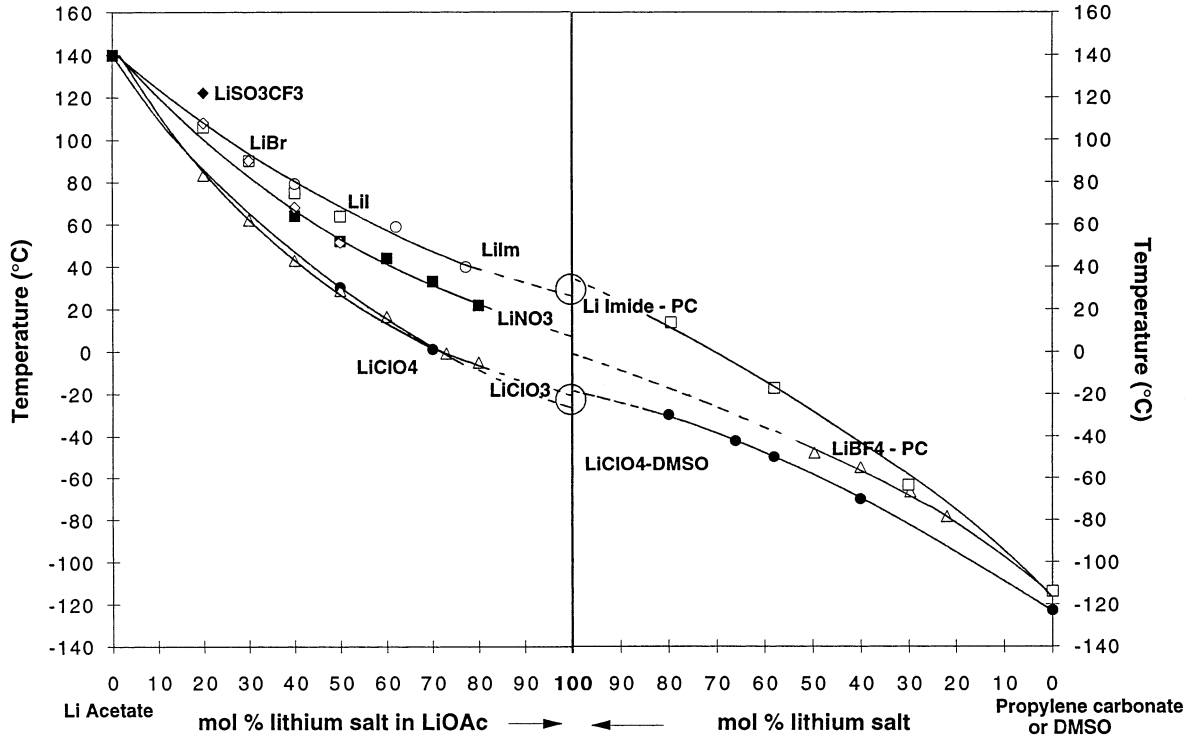

Figure 4. Plot of glass transition temperatures in binary salt solutions with a common component on the left (lithium acetate) and in binary solutions of the same second component in different nonaqueous solutions on the right. The plot permits comparisons of the extrapolations to pure liquid salts from two different solution regimes, thus helping to establish the plausibility of the extrapolated glass transition temperatures for individually nonglassforming substances.

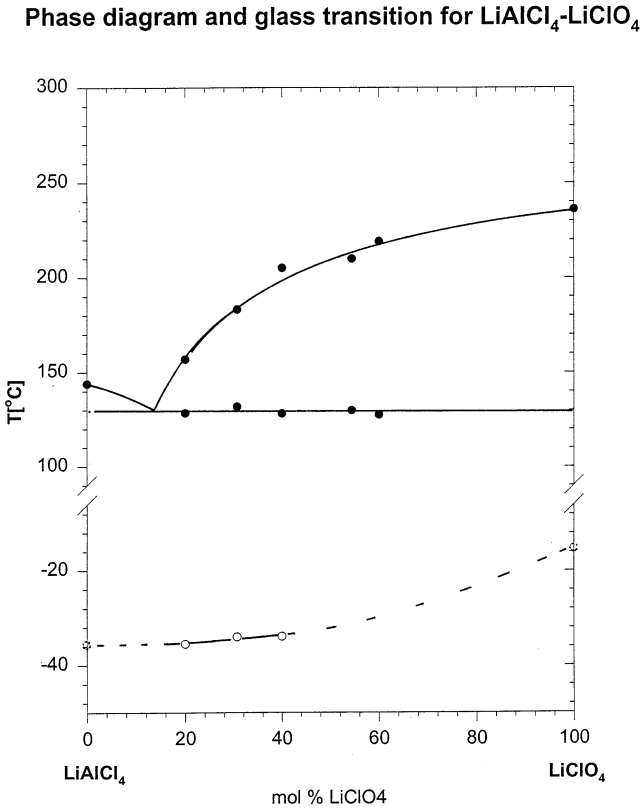

Figure 5. Phase diagram and glass transition temperature relationships for binary solutions of $LiClO_4$ and $LiAlCl_4$ showing extrapolation of T_g plot to pure $LiAlCl_4$.

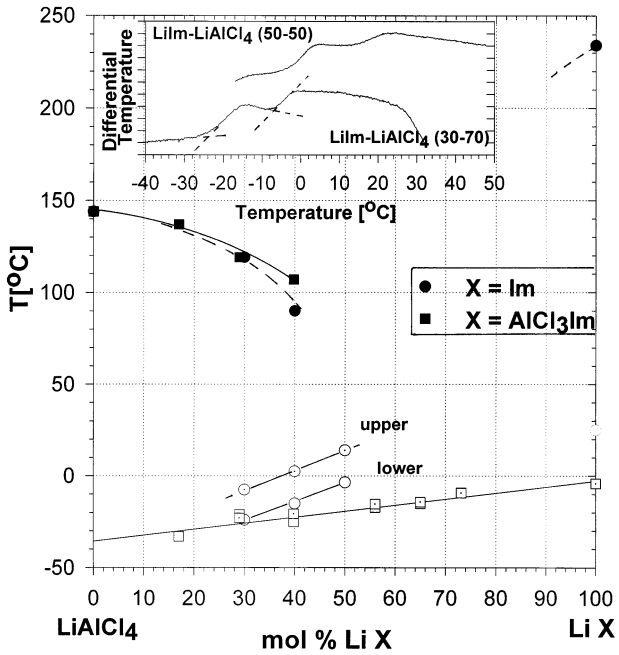

Figure 6. Phase diagram and twin glass transition temperatures in the systems (a) $LiAlCl_4$−Li imide ("imide" is bis (trifluoromethanesulfonyl) imide) (b) $LiAlCl_4$ − Li trichloroimidealuminate. Insert shows DSC scans with double glass transitions indicative of complex structure near T_g.

composition. Evidently $LiClO_4$ nucleates from the mixture less readily than does $LiAlCl_4$, hence can tolerate a greater supercooling before crystals begin to form. The glass transition temperatures are very low, reflecting the low T_g of the $LiAlCl_4$ component. It is clear that $LiAlCl_4$ has quite the lowest value of T_g of any of the salts investigated.

A wider range of glass-forming compositions exists in the $LiAlCl_4$−Li "imide" system ("imide" is bis-(trifluoromethane sulfonyl) imide). This is because, while Li imide has a melting point very similar to that of $LiClO_4$, its T_g is much higher, hence the melt is much more viscous at its freezing temperature. This is the principal characteristic of glass-forming systems. While the effect is not large enough to bestow glass-forming ability on Li imide itself, the additional melting point lowering associated with the formation of the binary solution allows crystallization to be by-passed easily for a considerable range of binary solutions.

The phase diagram for this system is shown in Figure 6 and the T_g values in the glass-forming range are included in the lower part of the figure. Note that the extrapolation to zero imide content gives a falsely low value for T_g of $LiAlCl_4$ implying that there is some sort of nonideality in the mixing thermodynamics of these two compounds in the liquid state. This is attributed to two factors: (i) the tendency of Li ions to remain associated with the imide nitrogen which interferes with the random mixing of anions across the quasi-lattice demanded by Temkin ideality for molten salt systems,[20] and (ii) a thermodynamic incompatibility of the highly fluorinated imide anion and the more polarizable $AlCl_4^-$ anion. The incompatibility is manifested by the double glass transition phenomenon seen in the DSC scans inserted in Figure 6. The double glass transition implies that microscopic liquid−liquid phase separation occurs near the glass transition temperature. This phenomenon is seen more vividly in aqueous systems[21] and will not be discussed in detail here.

To reduce these effects, and consequently to enhance the conductivity, the imide anion was converted to a sort of "tetraligand aluminate" by mixing 1:1 with $AlCl_3$. This melt achieves one of the objectives of our investigations in that it is a liquid lithium salt that does not crystallize—a rare material which we have called a lithium "ionic oil". Unfortunately, in this case it is an ionic oil of quite poor conductivity.

A binary system using this complex salt as a second component, $LiAlCl_4$ + $LiAlCl_3Im$, behaves in a more ideal manner than the uncomplexed imide system, if we judge by the almost linear behavior of T_g shown in Figure 6 and the suppression of the "split-T_g" effect. The data now extrapolate to the value $T_g = -35$ °C for $LiAlCl_4$ as suggested earlier by the data in Figure 5. The value of T_g for the trichloroimide aluminate salt is higher, which is not surprising since it is a massive anion. In the phase diagram for the new and ideal-mixing system, which is shown by dashed lines in Figure 6, only the liquidus curve on the $LiAlCl_4$-rich side of the diagram can be seen, because a eutectic temperature cannot be obtained unless two distinct crystalline phases cocrystallize.

The binary solutions of this system are stable enough to permit extended conductivity studies through the liquid range into the glassy state. The results of conductivity measurements are contained in Figure 7 where the data are shown in Arrhenius form. Strong departures from Arrhenius behavior typical of fragile liquids are evident. Figure 8 shows these data in the form of isotherms to show more clearly the composition dependence of the conductivity.

Discussion

The glassforming behavior and glass transition temperatures of the solutions of this study have been adequately discussed in the previous section. In this section we consider aspects of

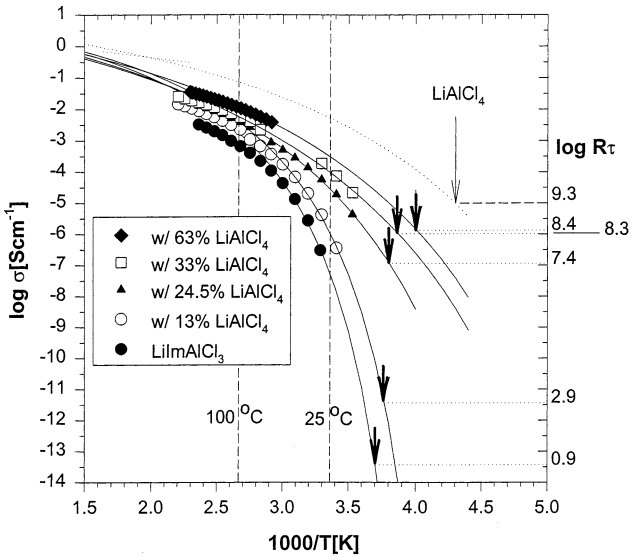

Figure 7. Arrhenius plots of the conductivity of solutions in the system $LiAlCl_4$ + Li trichloroimide aluminate. Arrows show position of the glass transition temperatures. The conductivity at T_g is used with eq 5 to obtain the log R_τ^* values scaled on the right-hand ordinate. The data are fitted (solid lines) by a Vogel−Fulcher law (eq 1) with the pre-exponent assigned the value log $\sigma_o = 1.0$) usually found for glassy Li^+-conducting systems[4] in order to avoid the distorting influence of ion pairing which sets in at the higher temperatures. Then Vogel−Fulcher temperatures which are physically reasonable ($T_o < T_g$, $T_g/T_o = 1.16$) are obtained, and the D value (5.5) indicates the fragility reliably. Dotted line shows behavior extrapolated for pure $LiAlCl_4$ using the Vogel−Fulcher law based on the literature data above the melting point, and a log R_τ value obtained from studies of a $LiAlCl_4 + LiAlI_4$ eutectic reported elsewhere.[31]

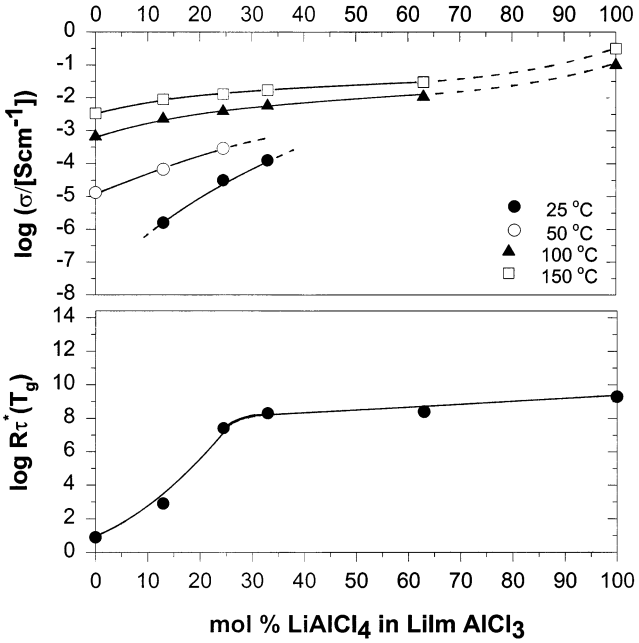

Figure 8. Composition dependences of (a) the conductivity for fixed temperatures between 25 and 150 °C, with extrapolations to values estimated for $LiAlCl_4$ using the Vogel−Fulcher extrapolation shown in Figure 7, and explained in the Figure 7 caption. (b) the decoupling index log R_τ^*, showing a saturation at about 33% $LiAlCl_4$. The break at 33.3% is suggestive of a percolation threshold and is probably related to the microphase separations indicated by Figure 6 (inset).

the conductivity phenomenology which we have neglected in recent accounts[1,22,23] of the conductivity of what might be called "superionic-conducting liquids".

There has been a tendency, in the treatment of ionic conductivity in glassforming systems, particularly in "solid polymer electrolytes", i.e., in solutions of salts in polyether solvents, to assign all deviations from Arrhenius behavior to the same source. This has often been considered to be a "free volume" effect, and therefore the raw conductivity data have been fitted to the conductivity form of the Vogel−Fulcher−Tammann equation (often designated "VTF equation"), eq 1, which was first justified by free volume arguments.[24]

The parameters obtained have frequently been unphysical insofar as the parameter T_o obtained has been close to, or higher than, the value of the glass transition temperature T_g measured at lower temperatures. According to any serious theoretical treatment of the non-Arrhenius viscosity behavior of glass-forming systems,[24,25] T_o, at which the viscosity diverges, must lie below T_g, the temperature where the viscosity merely reaches a high value associated with a relaxation time long enough to cause the loss of equilibrium ("ergodicity-breaking") recorded as T_g by scanning calorimetry.

If we proceed in the same manner with the present data, we obtain good numerical fits to the three-parameter equation, but with the same unphysical characteristics. In particular the pre-exponent for the conduction process would appear to be 4 orders of magnitude below the infrared conductivity ($\sim 10^1$ S cm^{-1}) which should be the value approached at high temperatures in the absence of complicating factors.[26] We believe the complicating factor is the tendency of the imide anion to form close ion pairs with the Li^+ as temperature increases. Comparable tendencies have been observed to occur in the case of polymer electrolytes.[27−30] In this case, while the diffusivity will continue to follow an eq 1 form, the conductivity will increase less rapidly and may even pass through a maximum.

To deal with this problem we adopt the following line of thought. Since we are most interested in obtaining information on decoupling and fragility, we factor out the ion pairing influence by assuming (on the basis of earlier experience[27−30]) that they affect mainly the high-temperature properties. Thus we assign an eq 2 pre-exponent σ_o typical of the fully dissociated melts, log (σ_o/S cm^{-1}) = 1, and then fit eq 1 to the low-temperature points. The T_o values obtained with this data treatment are physically sensible insofar as they fall below T_g for all compositions. The solid lines in Figure 7 are the best fit lines for this data-fitting procedure. It can be seen that the most important departures from the VFT equation are for the compositions highest in the trichloroimide aluminate anion, which is reasonable if the imide nitrogen is responsible for both ion pairing and coupling effects.

The position of the glass transition temperature is marked by an arrow in Figure 7 for each composition, and it can be seen that the decoupling of conductivity from viscosity rises rapidly with introduction of the tetrachloroaluminate anion. The values of log R_τ^* indicated in Figure 7 are plotted against mol % $LiAlCl_4$ in Figure 8. By 33% of the latter, the decoupling index is almost the same as for pure $LiAlCl_4$, for which the value is obtained by studies of a glassforming $LiAlCl_4 + LiAlI_4$ eutectic melt reported elsewhere.[31]

The T_o values obtained by this procedure are displayed in Figure 9 as open circles and discussed below.

According to this analysis the imide, even when complexed with $AlCl_3$, still provides fatal traps for the Li^+ cations, since the decoupling index (eq 1) is unity, in log units. A value like this, which is to be compared with values of log R_τ of 12 for superionic glasses,[4] implies essentially complete coupling of cations to anions. However, as seen in Figure 8b, the decoupling

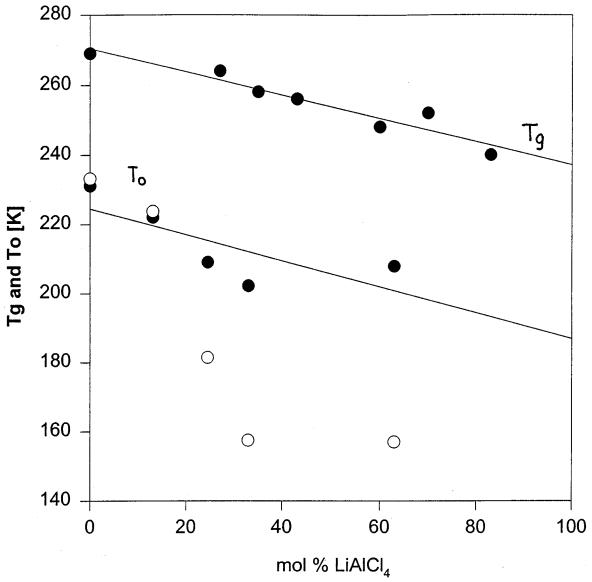

Figure 9. Comparison of glass transition temperatures and derived ideal glass transition (T_o of eq 1) values for $LiAlCl_4$−Li trichloroimide-aluminate solutions. The open symbols are fits subject to the restriction $\log \sigma_o = 1.0$. The closed symbols are obtained when the additional restriction to constant fragility ($D = 5.5$) is imposed. Data over a wider range of conductivity will be required to remove the ambiguities.

index increases rapidly as the mole fraction of $LiAlCl_4$ increases in the binary system, and reaches a value almost that estimated for $LiAlCl_4$ on addition of just 33% of $LiAlCl_4$. The break in R_τ is quite sharp and is suggestive of a percolation phenomenon, which it would be natural to assign to the percolation of $LiAlCl_4$-rich (large R_τ) regions of the liquid−liquid microphase structure referred to earlier in connection with the Figure 6 insert.

For the fully coupled case of pure $LiAlCl_3$·imide, the fragility can be obtained from the conductivity data, on the assumption that the viscosity relaxation time is 200 s at the glass transition temperature. The value obtained for D ($D = 5.5$) corresponds to a steepness index[32] of $m = 123$, or a $F_{1/2}$ fragility[33] of 0.79, which places these liquids among the most fragile on record. Such a value is supported by the very narrow glass transitions observed for these liquids. The reduced glass transition widths $\Delta T_g/T_g$[34] are comparable with those of the most fragile molecular liquids determined with the same apparatus.[33]

Free fitting of the remaining parameters T_o and D for the decoupled solution results in sharply lower fragilities, and T_o values, displayed in Figure 9 which are far below those anticipated from a smooth evolution of the T_o/T_g values. On the other hand if a constant fragility is assigned on the basis of the observed constant reduced width of the glass transition,[34] then the new T_o values (solid symbols) show slopes close to their T_g counterparts. The onset of decoupling has been seen in earlier work[35] to cause a return to Arrhenius behavior on the part of the conductivity which would then cause T_o to approach 0 K and accordingly give rise to of the apparent discrepancies. Details of this behavior will have to await studies of the viscosity temperature dependence.

Acknowledgment. This work has been supported by the DOE-BES program under Grant No. DEF9039ER45541, and by a Grant from Moltech Corporation.

References and Notes

(1) Angell, C. A.; Liu, C.; Sanchez, E. *Nature* **1993**, *362*, 137−139.
(2) (a) Xu, K.; Angell, C. A. *Symp. Mater. Res. Soc.* **1995**, 369, 505. (b) Angell, C. A.; Molten Salt Forum 1998; Wendt, H., Ed.; Vols. 5−6; 39−42.
(3) Moynihan, C. T.; Balitactac, N.; Boone, L.; Litovitz, T. A. *J. Chem. Phys.* **1971**, *55*, 3013.
(4) Angell, C. A. *Annu. Rev. Phys. Chem.* **1992**, *43*, 693; *Solid State Ionics* **1983**, *9 & 10*, 3.
(5) (a) Angell, C. A. *J. Phys. Chem. Sol.* **1988**, *49* (8), 863. (b) Angell, C. A. *J. Non-Cryst. Solids* **1991**, *131−133*, 13−31.
(6) (a) Vogel, H. *Physik. Z.* **1921**, *22*, 645. (b) Fulcher, G. S. *J. Am. Ceram. Soc.* **1925**, *8*, 339. (c) Tammann, V. G.; Hesse, W. *Z. Anorg. Allg. Chem.* **1926**, *156*, 245.
(7) Angell, C. A.; Ngai, K. L.; McKenna, G. B.; McMillan, P. F.; Martin, S. W. *Rev. Appl. Phys.*, to be published.
(8) Angell, C. A. *J. Res. NIST* **1997**, *102*, 171.
(9) Angell, C. A.; Bressel, R. D. *J. Phys. Chem.* **1972**, *76*, 3244.
(10) Angell, C. A.; Rao, K. J. *J. Chem. Phys.* **1972**, *57*, 470−481.
(11) Angell, C. A.; Richards, B. E.; Velikov, V. *J. Phys.: Condens. Matter*, in press.
(12) (a) Biltz, W.; Klemm, W. *Z. Anorg. Allg. Chem.* **1926**, *152*, 267. (b) Pugsley, F. A.; Westmore, F. E. W. *Can. J. Chem.* **1954**, *32*, 839.
(13) (a) Angell, C. A.; Moynihan, C. T. *Molten Salts; Characterization and Analysis*; Mamantov, G., Ed.; Marcel Dekker: New York, June 1969; p 315. (b) Moynihan, C. T.; Smalley, C. R.; Angell, C. A.; Sare, E. J. *J. Phys. Chem.* **1969**, *73* (6), 2287.
(14) Ingram, M. D. *Mater. Chem. Phys.* **1989**, *23*, 51.
(15) Pradel, A.; Ribes, M. *Mater. Chem. Phys.* **1989**, *23*, 121.
(16) Kincs, J.; Martin, S. W. *Phys. Rev. Lett.* **1996**, *76*, 70.
(17) See the volume of workshop papers in *Solid State Ionics* **1997**, *105*.
(18) Moynihan, C. T.; Macedo, P. B.; Montrose, C. J.; Gupta, P. K.; DeBolt, M. A.; Dill, J. F.; Dom, B. E.; Drake, P. W.; Easteal, A. J.; Elterman, P. B.; Moeller, R. P.; Sasabe, H. A.; Wilder, J. A. *Ann. N.Y. Acad. Sci.* **1976**, *279*, 15.
(19) Zhang, S.-S.; Angell, C. A. *J. Electrochem. Soc.* **1996**, *143*, 4047.
(20) Temkin, M. *Acta Phys. Chim. SSSR* **1945**, *20*, 411.
(21) Velikov, V.; Angell, C. A. To be published.
(22) Fan, J.; Marzke, R. F.; Sanchez, E.; Angell, C. A. *J. Non-Cryst. Solids* **1994**, *172−174*, 1178−1189.
(23) Angell, C. A.; Fan, J.; Liu, C.; Sanchez, E.; Xu, K. *Solid State Ionics*, **1994**, *69*, 343−353.
(24) Cohen, M. H.; Turnbull, D. *J. Chem. Phys.* **1959**, *31*, 1164.
(25) Adam, G.; Gibbs, J. H. *J. Chem. Phys.* **1965**, *43*, 139.
(26) Liu, C.; Angell, C. A. *J. Chem. Phys.* **1990**, *93*, 7378.
(27) Wintersgill, M. C.; Fontanella, J. J.; Pak, Y. S.; Greenbaum, S. G.; Al-Mudaras, A.; Chadwick, A. V. *Polymer* **1989**, 1123.
(28) It is notable that when the conductivity is controlled by ions dissolved in the PEO component of a block PPO−PEO copolymer, the pre-exponent becomes comparable with that in molten salts, i.e., ion pair formation does not develop at high temperatures. (Xue, R.; Angell, C. A. *Solid State Ionics* **1987**, *25*, 223).
(29) Kakihana, M.; Schantz, S. ; Torell, L. M. *J. Chem. Phys.* **1990**, *92*, 6271.
(30) McLin, M. C.; Angell, C. A. *J. Phys. Chem.* **1991**, *95*, 9464.
(31) Lucas, P.; Angell, C. A. To be published.
(32) Plazek, D. J.; Ngai, K. L. *Macromolecules* **1991**, *24*, 1222.
(33) (a) Richert, R.; Angell, C. A. *J. Chem. Phys.* **1998**, *108*, 9016. (b) Green, J. L.; Ito, K.; Xu, K.; Angell, C. A. *J. Phys. Chem.*, in press.
(34) Ito, K.; Angell, C. A.; Moynihan, C. T. *Nature*, in press.
(35) Howells, F. S.; Bose, R. A.; Macedo, P. B.; Moynihan, C. T. *J. Phys. Chem.* **1974**, *78*, 639.